

Probing the shape of the quark-gluon plasma droplet via event-by-event QGP tomography

Bithika Karmakar

*Institute of Physics Belgrade, University of Belgrade, Serbia and
Incubator of Scientific Excellence—Centre for Simulations
of Superdense Fluids, University of Wrocław, Poland*

Dusan Zigic and Magdalena Djordjevic

Institute of Physics Belgrade, University of Belgrade, Serbia

Pasi Huovinen

*Incubator of Scientific Excellence—Centre for Simulations
of Superdense Fluids, University of Wrocław, Poland*

Marko Djordjevic

Faculty of Biology, University of Belgrade, Serbia

Jussi Auvinen*

University of Jyväskylä, Finland

This study investigates Quark-Gluon Plasma (QGP) in heavy-ion collisions through two avenues: high- p_{\perp} frameworks and hydrodynamic modeling. Using the T_RENTo model, we find that IP-Glasma mimicking $p = 0$ value aligns well with high- p_{\perp} data, in agreement with Bayesian analysis of the low- p_{\perp} regime. While adjusting p values may improve a fit to a particular high- p_{\perp} observable, it does not permit an earlier onset of transverse expansion.

I. INTRODUCTION

A new state of matter, called Quark-Gluon Plasma (QGP), consisting of deconfined but interacting quarks, antiquarks, and gluons, is formed in ultra-relativistic heavy ion collisions at

* E-mail: jussi.a.m.auvinen@jyu.fi

the Relativistic Heavy Ion Collider (RHIC) and the Large Hadron Collider (LHC) experiments [1–4]. These collisions create an expanding fireball of quarks and gluons, which thermalizes to form QGP and eventually hadronizes. Extracting useful information about the properties of QGP formed in these collisions from the measured particle distributions, requires comparing theoretical predictions with the data, using phenomenological models describing the evolution of the collision system. In particular fluid-dynamical models have been very successful in describing a large amount of the low- p_\perp data.

Fluid-dynamical models do not provide the initial state of the fluid-dynamical evolution, but it must be provided by some other model, or parametrization. This ambiguity causes significant uncertainty in the properties of QGP extracted from the data (see e.g. Ref [5].) Recently, Bayesian analyses of the data have significantly reduced this uncertainty by showing that the data strongly favors initial entropy deposition proportional to the geometric mean of the local nuclear thickness function [6, 7]. Such proportionality corresponds to the value of the p parameter of the T_RENTo model [8] being approximately zero, and is consistent with the state-of-the-art IP-Glasma [9, 10] and EKRT [11–13] models for initial particle production. However, these analyses are based on low- p_\perp particles, most of which leave the system at the very end of the evolution, and thus reflect its properties at the late stage. High- p_\perp particles formed in the primary nucleus-nucleus collisions, on the other hand, leave the system during the first few fm/ c of its evolution, and probe the initial stages of the system more directly than low- p_\perp particles. Therefore, it is important to study whether the high- p_\perp observables, R_{AA} and flow harmonics v_2 , v_3 , and v_4 , favor the same initial shape of the fireball as the low- p_\perp particles.

Furthermore, in our previous works [14, 15] we found that the high- p_\perp observables can be reproduced only if the transverse expansion is very weak (or nonexistent) until $\tau \approx 1$ fm, but the Bayesian analyses using the T_RENTo model usually assume immediate transverse expansion after the primary collisions in terms of free-streaming [6, 7]. This brings into question whether delaying transverse expansion until $\tau_0 = 1$ fm will change the shape favored by the data. As well, the requirement of late onset of transverse expansion was based on conventionally shaped initial states corresponding to the $p \approx 0$ value. Thus, it is possible that if the initial state was way more anisotropic than commonly assumed, transverse expansion could begin earlier, and high- p_\perp anisotropies would still be reproduced.

In this work, we address these two issues: We modulate the initial shape of the system by altering the T_RENTo parameter p while adjusting the other parameters to reproduce a subset

of the low- p_\perp data. We do not allow transverse expansion before the onset of fluid-dynamical evolution at $\tau_0 = 1$ fm, calculate the high- p_\perp observables for each value of p , and compare with the data to see which value, and thus shape, the data favor. We also systematically decrease the p -value down to $p = -3$ to select more anisotropic initial distribution and carry out calculations using $\tau_0 = 0.6$ fm and $\tau_0 = 0.2$ fm to see if highly anisotropic initial state would lead to large enough high- p_\perp anisotropies even if the early transverse expansion diluted a large part of the spatial anisotropy by the time the jets become sensitive to it.

II. METHODS

A. Bulk medium evolution

To generate the event-by-event fluctuating initial entropy profiles, we use the phenomenological model T_RENTo [8], which produces the initial profiles without assuming any specific mechanism for entropy production. Instead, the starting point is the so-called thickness function of the colliding nuclei A and B

$$\tilde{T}_{A,B}(x, y) = \int dz \rho_{A,B}^{\text{part}}(x, y, z), \quad (1)$$

where $\rho_{A,B}^{\text{part}}$ is the density of the nuclear matter that participates in the inelastic collisions. In event-by-event case it is calculated by sampling the Woods-Saxon distribution to create the positions of nucleons, which are described as Gaussian distributions. For this process, we use the parameters from Ref. [16]: width $w = 0.5$ fm, minimum nucleon-nucleon distance $d = 0.5$ fm, inelastic nucleon-nucleon cross section $\sigma_{NN} = 7$ fm² and fluctuation parameter $k = 1.19$. The initial entropy density is related to the thickness functions as

$$s(x, y) \propto \tilde{T}_R(p; \tilde{T}_A, \tilde{T}_B) \equiv \left(\frac{\tilde{T}_A^p + \tilde{T}_B^p}{2} \right)^{1/p}, \quad (2)$$

where p is a continuous parameter which can have values from $-\infty$ to ∞ . As known, T_RENTo can be used to mimic and interpolate between various initial state models; the values of $p = -2/3, 0$ and 1 corresponding to KLN, EKRT/IP-Glasma, and wounded nucleon models, respectively. In this study, however, we consider p a free parameter that allows us to test different shapes of the initial state. In particular, we use $p \in \{1/3, 0, -1/3, -2/3, -1, -3\}$ to see which value the high- p_\perp data favors and whether higher initial anisotropy would allow the earlier onset of transverse expansion.

	$\tau_0 = 1$ fm						$\tau_0 = 0.6$ fm		$\tau_0 = 0.2$ fm	
p	1/3	0	-1/3	-2/3	-1	-3	0	-3	0	-3
η/s	0.03	0.15	0.18	0.20	0.25	0.29	0.17	0.33	0.20	0.60

TABLE I: η/s values used for each value of p and initial time τ_0

We do not allow any pre-equilibrium evolution (free-streaming or otherwise). In the first part of the study, we use $\tau_0 = 1$ fm as the initial time for fluid-dynamical evolution with zero transverse velocity since the reproduction of the high- p_\perp observables does not allow strong transverse expansion earlier [14]. In the second part of the study, we use $\tau_0 = 0.6$ fm and $\tau_0 = 0.2$ fm to test whether large anisotropy would allow the earlier onset of transverse expansion.

We evolve the event-by-event fluctuating initial distributions using the version of VISH-New [17, 18] used in Refs. [6, 19, 20][50]. This code solves the dissipative fluid-dynamical equations in 2+1-dimensions, i.e., assuming boost invariance. Shear stress and bulk pressure are taken as dynamical variables and evolved according to the Israel-Stewart type equations [22]. We use an Equation of State (EoS) [19] that combines the lattice QCD-based EoS of the HotQCD collaboration [23] at large temperatures to a hadron resonance gas EoS at low temperatures. The fluid is particlized on an isothermal hypersurface of $T_{\text{sw}} = 151$ MeV using the Cooper-Frye prescription [24], and the particles fed to the UrQMD hadron cascade [25, 26], which describes the evolution of the hadronic stage of the system.

The temperature dependence of the specific bulk viscosity is parameterized as a Cauchy distribution [20] with the maximum value $(\zeta/s)_{\text{max}} = 0.03$, and the other parameters characterizing the bulk viscosity being the same as in Ref. [16]. Instead of allowing temperature-dependent specific shear viscosity, we use constant η/s , since in our earlier study [16] we found that the high- p_\perp observables could be equally well reproduced using constant η/s as temperature dependent η/s .

We keep all the other parameters fixed but adjust the T_RENTo normalization parameter and η/s for each value of the p parameter to reproduce the charged particle elliptic flow $v_2\{4\}$, and proton, pion and kaon multiplicities in each centrality class. The required values of η/s are shown in Table I.

We generate 10^4 events for each T_RENTo p value. These events are then sorted into centrality bins according to the number of participants in the collision. We analyze the events in four centrality classes, 10-20%, 20-30%, 30-40%, and 40-50%, where the low- p_\perp observables are cal-

culated for each event and averaged over the events in the class. Subsequently, the temperature profiles in each centrality class are used as input to the generalized DREENA-A to calculate the high- p_\perp observables in each class.

B. Generalized DREENA-A framework

In our study, the high- p_\perp energy loss has been computed using the DREENA-A (Dynamical Radiative and Elastic ENergy loss Approach) framework where ‘A’ stands for Adaptive, *i.e.*, arbitrary temperature profile can be included as input in this framework. This has been further optimized to incorporate event-by-event fluctuations in the temperature profiles. The framework is based on generalized hard thermal loop perturbation theory [27] in which the infrared divergences are naturally regulated [28, 29]. It has several important features that make it a reliable tool for QGP tomography: i) The system is considered as finite size dynamical medium *i.e.*, it consists of moving partons, ii) Both the radiative [30, 31] and collisional [28] energy loss have been computed within the same framework, iii) It is generalized to include the running coupling [32], finite magnetic mass [33], and beyond soft-gluon approximation [29]. iv) It does not have fitting parameters in the energy loss, *i.e.*, all the parameters are set to standard literature values [14, 34], allowing systematic comparison of data and the predictions from the simulation obtained using the same formalism and parameter set. We recently also extended the formalism to include finite orders in opacity [35] but found out that including these effects has a minor impact on high- p_\perp predictions. Thus, a computationally more efficient version with one scattering center is used in this study.

To generate the medium-modified distribution of high- p_\perp particles, we use the following pQCD convolution formula:

$$\frac{E_f d^3\sigma_q(H_Q)}{dp_f^3} = \frac{E_i d^3\sigma(Q)}{dp_i^3} \otimes P(E_i \rightarrow E_f) \otimes D(Q \rightarrow H_Q), \quad (3)$$

where i and f denote the initial parton (Q) and the final hadron (H_Q) respectively. $\frac{E_i d^3\sigma(Q)}{dp_i^3}$ represents initial parton spectrum that is calculated in accordance with Ref. [36–38]. As discussed above, the energy loss probability $P(E_i \rightarrow E_f)$ has been computed within finite temperature field theory. $D(Q \rightarrow H_Q)$ represents the fragmentation function, where DSS, BCFY, and KLP fragmentation functions have been used for light hadrons, D, and B mesons, respectively. We consider the gluon mass $m_g = \mu_E/\sqrt{2}$ [39] where μ_E is the temperature-dependent Debye mass

that is calculated following the procedure in Ref. [40]. Further, we assume the mass of the light quark, charm, and bottom quark to be $M = \mu_E/6$, 1.2 GeV, and 4.75 GeV, respectively. The magnetic to electric mass ratio is $\mu_M/\mu_E = 0.6$ [41]. Also, we assume $\Lambda_{QCD} = 0.2$ GeV and effective number of light quark flavors $n_f = 3$ in our study.

III. RESULTS

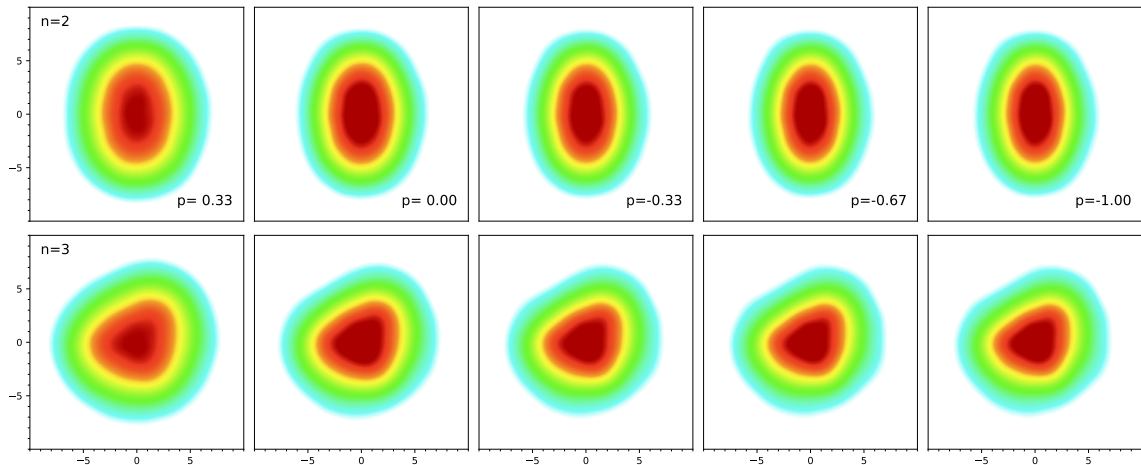


FIG. 1: The averaged initial ($\tau = 1$ fm) temperature distributions for $p \in \{1/3, 0, -1/3, -2/3, -1\}$ at 20-30% centrality. When averaging, the participant angles of each event were aligned. The distributions in the upper row were aligned with respect to the $\Psi_{2,2}$ angle, and in the lower row w.r.t. $\Psi_{2,3}$, making the average ellipticity and triangularity visible.

We characterise the initial state anisotropies with the coefficients $\epsilon_{m,n}$ [42]

$$\epsilon_{m,n} = -\frac{\int dxdy r^m \cos[n(\phi - \Psi_{m,n})] e(x, y)}{\int dxdy r^m e(x, y)} \quad (4)$$

where (r, ϕ) are the radial coordinates in the transverse plane, $e(x, y)$ is the energy density and $\Psi_{m,n}$ is the event plane angle:

$$\Psi_{m,n} = \frac{1}{n} \arctan \frac{\int dxdy r^m \sin(n\phi) e(x, y)}{\int dxdy r^m \cos(n\phi) e(x, y)} + \pi/n. \quad (5)$$

To illustrate how the shape of the initial state depends on the parameter p , we show in Fig. 1 the averaged initial temperature distributions at 20-30% centrality for various values of p , and the anisotropy parameters $\epsilon_{2,2}$ and $\epsilon_{2,3}$ as function of p at various centralities in Fig. 2. When

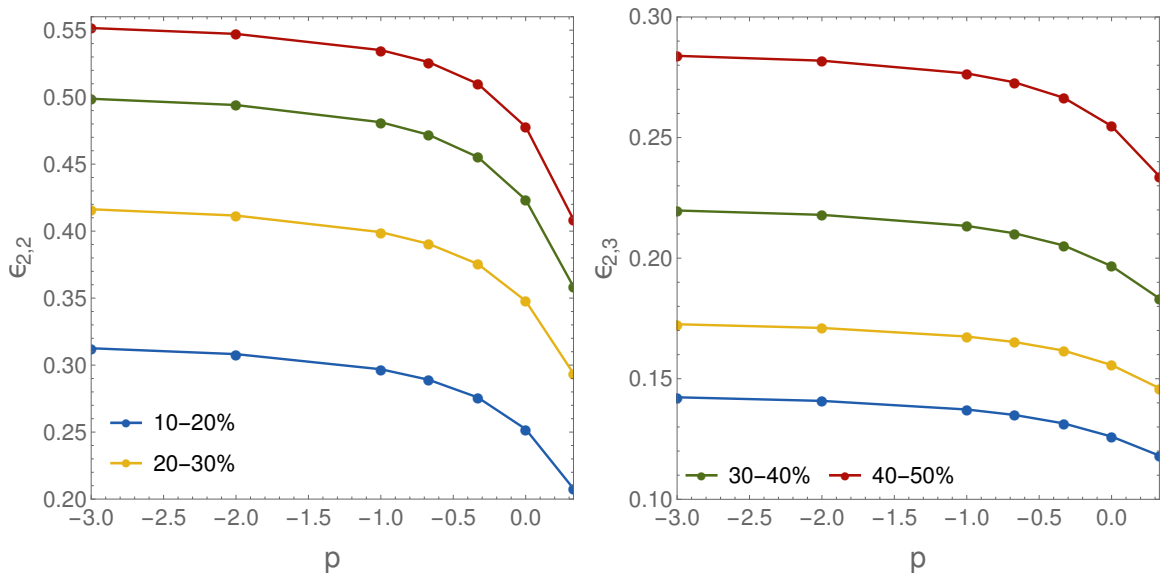


FIG. 2: The anisotropy parameters $\epsilon_{2,2}$ and $\epsilon_{2,3}$ as function of p at various centralities.

averaging, the individual events were rotated to align their participant angles $\Psi_{2,2}$ (upper row of Fig. 1) or $\Psi_{2,3}$ (lower row of Fig. 1) to make the average ellipticity (upper row) or triangularity (lower row) visible. As seen, the system becomes more elliptically elongated and more triangular when p is reduced.

At low p_{\perp} , the v_2 and v_3 are strongly correlated with their corresponding spatial anisotropies [42], but at high p_{\perp} their behavior is more complicated. This can be seen in Figs. 3 and 4, where we show the calculated R_{AA} and high- p_{\perp} v_2 , v_3 and v_4 at 20-30% and 40-50% centrality, respectively. These results are for Pb+Pb collisions at $\sqrt{s_{NN}} = 5.02$ TeV, and compared with the data. When p is non-negative, high- p_{\perp} v_2 increases with decreasing p , i.e., with increasing $\epsilon_{2,2}$, but once p becomes negative v_2 hardly changes even if $\epsilon_{2,2}$ keeps increasing. On the other hand, high- p_{\perp} v_3 is anticorrelated with $\epsilon_{2,3}$ and tends to decrease when $\epsilon_{2,3}$ increases (i.e., when p decreases), although when p is non-negative, v_3 hardly changes. This is surprising, but one has to keep in mind that the high- p_{\perp} anisotropies are not as sensitive to the initial shape of the system as they are to the time-average of the shape and the temperature of the system. Thus, at high p_{\perp} , we should not expect v_2 nor v_3 to be directly related to the eccentricities $\epsilon_{2,2}$ and $\epsilon_{2,3}$. Furthermore, as we have noted earlier [34], the high- p_{\perp} observable which reflects the shape of the system best is not v_2 , but the ratio $v_2/(1 - R_{AA})$.

The R_{AA} hardly depends on the shape of the system, but as we have discussed previously [34], the initial temperature where the energy loss sets in dominates R_{AA} . The p value does not directly

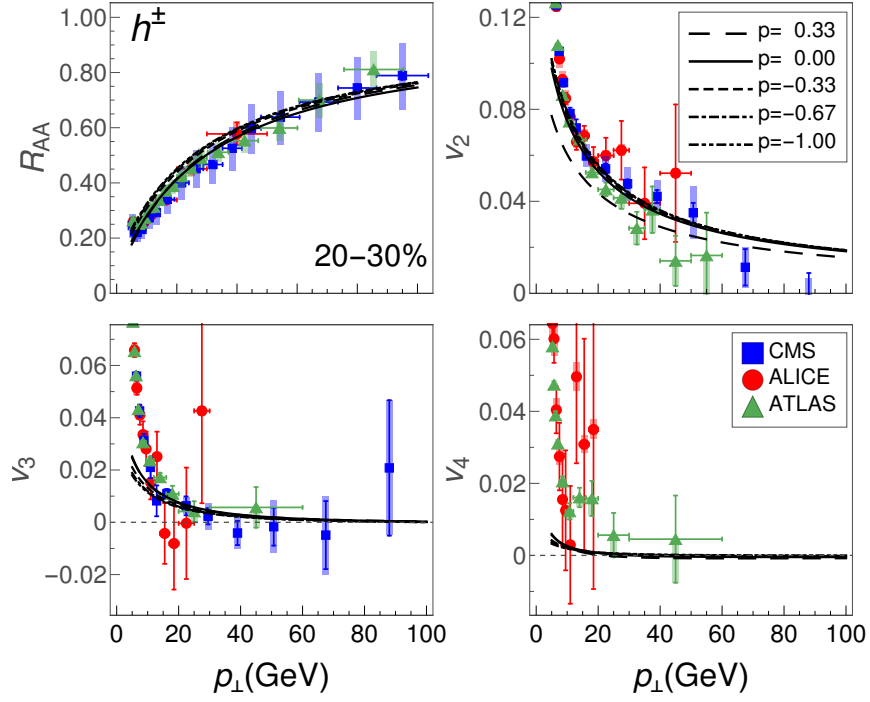


FIG. 3: The charged hadron R_{AA} and high- p_{\perp} flow harmonics v_2 , v_3 and v_4 as function of transverse momentum in Pb+Pb collisions at $\sqrt{s_{NN}} = 5.02$ TeV for different initializations at 20-30% centrality. CMS (blue squares) [43, 44], ALICE (red circles) [45, 46], and ATLAS (green triangles) [47, 48] experimental data are also shown for comparison.

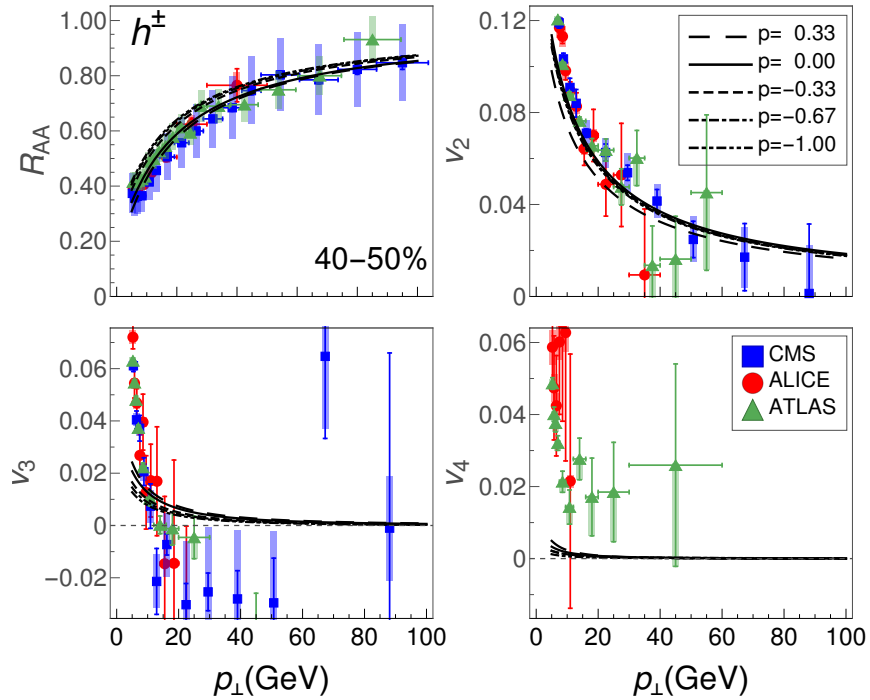


FIG. 4: The same as Fig. 3, but at 40-50% centrality.

affect the initial temperature, but since we require our calculations to reproduce the observed multiplicity and $v_2\{4\}$, we have to adjust the initial temperature accordingly. As seen in Fig. 1, the smaller the p , the smaller the system. Reaching the same final multiplicity necessitates a larger initial entropy density and, thus, higher temperature. On the other hand, the high initial eccentricity necessitates higher shear viscosity to dampen the low- p_\perp v_2 . Higher viscosity leads to higher entropy production during the evolution, and to obtain the same final multiplicity, the initial entropy density and, thus, temperature should be smaller. These two opposing trends do not quite cancel each other but lead to the overall tendency of initial temperature increasing with increasing p . The calculated R_{AA} , shown in the upper left panels of Figs. 3 and 4, generally follows the behavior of initial temperature: the larger the p the lower the R_{AA} . Based on these observations and comparison with the data[51], we can say that the observed R_{AA} and v_3 favors values $p \gtrsim 0$, whereas high- p_\perp v_2 favors values $p \lesssim 0$. Thus, we conclude that the high- p_\perp data favors the value $p \approx 0$ in agreement with the low- p_\perp data [6].

In contrast to the previous observables, the high- p_\perp v_4 is almost insensitive to the p value (lower right panels of Figs. 3 and 4). Furthermore, our generalized DREENA-A framework consistently underpredicts the experimental data for charged hadron v_4 . This discrepancy has been previously highlighted in our earlier works [16, 49], where variations in initial conditions, including the presence or absence of initial transverse free streaming, and different shear viscosity-to-entropy density (η/s) parametrizations led to similarly low predictions for high- p_\perp v_4 . We have called this divergence between theory and experiment the "high- p_\perp v_4 puzzle" [49].

Our comprehensive analyses demonstrate that attempts to resolve this puzzle through modifying parameters in fluid dynamical simulations—including eliminating free streaming, delaying thermalization time, employing diverse η/s parametrizations, or varying the p values for initial conditions—have yielded negligible impact on high- p_\perp v_4 . If upcoming high-luminosity experimental data corroborate these observations, resolving the v_4 puzzle might necessitate alternative approaches to initial state and/or energy loss models.

As known, the heavy quark energy loss is more sensitive to the details of the evolution of the fireball than the light quark energy loss. Therefore, we have also evaluated the R_{AA} and high- p_\perp anisotropies of D and B mesons shown in Fig. 5. The overall behavior is the same as for charged hadrons, but in particular v_3 becomes more sensitive to the initial anisotropy, and is able to differentiate between all values of p we tested. This enhanced sensitivity to details of

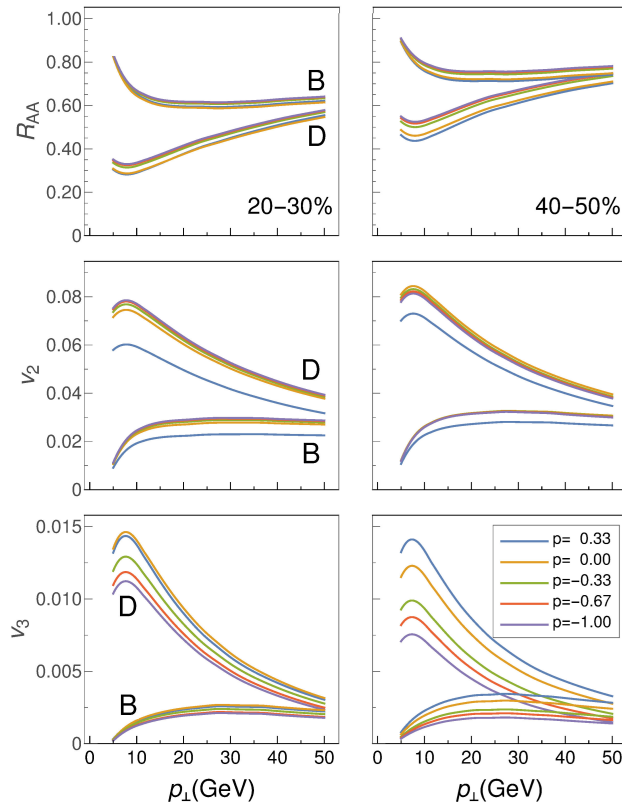


FIG. 5: The D and B meson R_{AA} (first row) and high- p_{\perp} flow harmonics v_2 (second row) and v_3 (third row) as function of transverse momentum in Pb+Pb collisions at $\sqrt{s_{NN}} = 5.02$ TeV for different initializations. The left column depicts collisions at 20-30% centrality and the right column at 50-60% centrality.

the evolution hints at the possibility that once the high-luminosity data becomes available from sPHENIX and Run 3 at the LHC, the study of D and B meson anisotropies may reveal structures so far hidden, and which the T_RENTo model cannot describe.

As discussed in the Introduction, we had observed in our earlier works that the reproduction of high- p_{\perp} v_2 is possible only if the transverse expansion of the fireball is delayed to $\tau \approx 1$ fm [14]. To study whether it would still be possible to start transverse expansion earlier and fit the v_2 data if the initial anisotropy was way larger than usually assumed, we cranked the p parameter of the T_RENTo model down to -3, and readjusted viscosity and normalization to reproduce the low- p_{\perp} data. The resulted high- p_{\perp} observables, R_{AA} , v_2 and v_3 of charged hadrons, are shown in Fig. 6. A comparison of the solid blue ($p = 0$ and $\tau_0 = 1$ fm) and dashed orange ($p = -3$ and $\tau_0 = 1$ fm) curves reveals behavior similar to previously discussed: Smaller p reduces temperature and

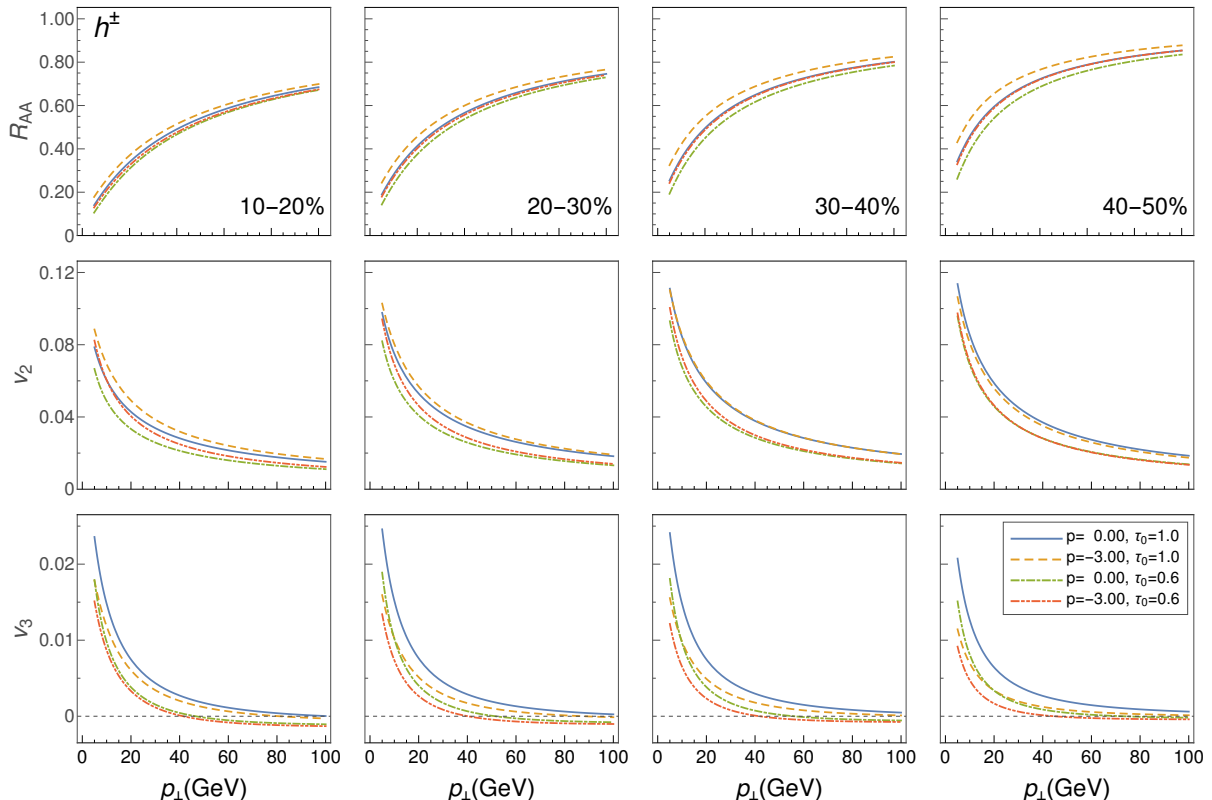


FIG. 6: Calculated charged hadron R_{AA} (first row), high- p_\perp v_2 (second row) and v_3 (third row) as function of transverse momentum for $p = 0$ and -3 and $\tau_0 = 1$ and 0.6 fm at 10-20%, 20-30%, 30-40% and 40-50% centrality classes.

increases both elliptic and triangular anisotropies. Consequently R_{AA} and v_2 increase whereas v_3 decrease. Interestingly, the increase in R_{AA} might allow an earlier start of energy loss without reducing R_{AA} too much. The red curve ($p = -3$ and $\tau_0 = 0.6$ fm) reveals this to be the case. R_{AA} is almost identical to R_{AA} obtained using $p = 0$ and $\tau_0 = 1$ fm, but the increase in v_2 is insufficient to compensate for the reduction due to the earlier onset of transverse expansion. Furthermore, both small p and early onset of expansion reduce v_3 , leading to smaller v_3 than experimentally observed. To be sure of our conclusions, we repeated the calculations using $p = -1$ and -2 , and obtained results which were between the ones obtained using $p = 0$ and $p = -3$. One could ask what would happen if we cranked p down even further, say, down to minus eleven, but as shown in Fig. 2, once $p \lesssim -2$, the anisotropies change very little. Therefore, we dare to conclude that if there is an initial state which is anisotropic enough to allow both early onset of transverse expansion and reproduction of high- p_\perp anisotropies, it cannot be modeled using T_RENTo.

As mentioned in the Introduction and Section IIA, we repeated this study using an even earlier start of transverse expansion and jet energy loss at $\tau = 0.2$ (results not shown), and it was even clearer that the increased anisotropy was insufficient to compensate for the reduction of R_{AA} and high- p_\perp v_2 due to early onset of expansion and energy loss [52].

IV. SUMMARY

In the fluid-dynamical models of heavy-ion collisions, the initial state is conventionally constrained by comparison to low- p_\perp data. In this study, we have provided a complementary approach by using high- p_\perp data, i.e., QGP tomography, to constrain the initial state. In particular, we carried out two distinct investigations:

i) We modulated the shape of the initial state by varying the parameter p of the T_RENTo model. We found out that while R_{AA} and v_3 preferred values $p \gtrsim 0$, high- p_\perp v_2 preferred $p \lesssim 0$. Thus, the best overall fit was obtained with $p \approx 0$, consistently with the Bayesian analysis of low- p_\perp data.

ii) We tested if larger elliptic anisotropy of the initial state, i.e., $p \ll 0$ would allow an earlier onset of transverse, in our case fluid-dynamical, expansion. Our results show that, while lower p values enhance high- p_\perp R_{AA} and v_2 , the enhancement is insufficient for facilitating an earlier onset of transverse expansion in heavy-ion collisions.

We conclude by noting that by providing a complementary approach to constrain the early stages of heavy-ion collisions, this research demonstrates the value of employing jet tomography, in which both low- and high- p_\perp theoretical and experimental data are collectively utilized to refine our understanding of QGP properties.

Acknowledgements: This work is supported by the European Research Council, grant ERC-2016-COG: 725741, and by the Ministry of Science and Technological Development of the Republic of Serbia. PH and BK were also supported by the program Excellence Initiative—Research University of the University of Wrocław of the Ministry of Education and Science. JA acknowledges the financial support from the Academy of Finland Project No. 330448. JA’s research was also funded as a part of the Center of Excellence in Quark Matter of the Academy of Finland (Project No. 346325). This research is part of the European Research Council Project No.

-
- [1] E. V. Shuryak, Nucl. Phys. A **750**, 64 (2005); Rev. Mod. Phys. **89**, 035001 (2017).
 - [2] M. Gyulassy and L. McLerran, Nucl. Phys. A **750**, 30 (2005).
 - [3] B. Jacak and P. Steinberg, Phys. Today **63**, 39 (2010).
 - [4] B. Muller, J. Schukraft and B. Wyslouch, Ann. Rev. Nucl. Part. Sci. **62**, 361 (2012).
 - [5] H. Song, S. A. Bass, U. Heinz, T. Hirano and C. Shen, Phys. Rev. Lett. **106**, 192301 (2011) [erratum: Phys. Rev. Lett. **109**, 139904 (2012)].
 - [6] J. E. Bernhard, J. S. Moreland and S. A. Bass, Nature Phys. **15**, no.11, 1113-1117 (2019).
 - [7] G. Nijs, W. van der Schee, U. Gürsoy and R. Snellings, Phys. Rev. C **103**, 054909 (2021).
 - [8] J. S. Moreland, J. E. Bernhard and S. A. Bass, Phys. Rev. C **92**, 011901 (2015).
 - [9] B. Schenke, P. Tribedy and R. Venugopalan, Phys. Rev. Lett. **108**, 252301 (2012).
 - [10] B. Schenke, P. Tribedy and R. Venugopalan, Phys. Rev. C **86**, 034908 (2012).
 - [11] K. J. Eskola, K. Kajantie, P. V. Ruuskanen and K. Tuominen, Nucl. Phys. B **570**, 379 (2000).
 - [12] R. Paatelainen, K. J. Eskola, H. Holopainen and K. Tuominen, Phys. Rev. C **87**, 044904 (2013).
 - [13] R. Paatelainen, K. J. Eskola, H. Niemi and K. Tuominen, Phys. Lett. B **731**, 126 (2014).
 - [14] S. Stojku, J. Auvinen, M. Djordjevic, P. Huovinen and M. Djordjevic, Phys. Rev. C **105**, L021901 (2022).
 - [15] S. Stojku, J. Auvinen, M. Djordjevic, M. Djordjevic and P. Huovinen, Acta Phys. Polon. Supp. **16**, no.1, 1-A156 (2023).
 - [16] B. Karmakar, D. Zigic, I. Salom, J. Auvinen, P. Huovinen, M. Djordjevic and M. Djordjevic, Phys. Rev. C **108**, 044907 (2023).
 - [17] H. Song and U. W. Heinz, Phys. Rev. C **77**, 064901 (2008).
 - [18] H. Song and U. W. Heinz, Phys. Rev. C **78**, 024902 (2008).
 - [19] J. E. Bernhard, J. S. Moreland, S. A. Bass, J. Liu and U. Heinz, Phys. Rev. C **94**, 024907 (2016).
 - [20] J. E. Bernhard, [arXiv:1804.06469 [nucl-th]].
 - [21] <https://github.com/Duke-QCD/hic-eventgen>
 - [22] W. Israel and J. M. Stewart, Annals Phys. **118**, 341-372 (1979).
 - [23] A. Bazavov *et al.* [HotQCD], Phys. Rev. D **90**, 094503 (2014).
 - [24] F. Cooper and G. Frye, Phys. Rev. D **10**, 186 (1974).

- [25] S. A. Bass *et al.* Prog. Part. Nucl. Phys. **41**, 255-369 (1998).
- [26] M. Bleicher *et al.* J. Phys. G **25**, 1859-1896 (1999).
- [27] J. I. Kapusta, “Finite Temperature Field Theory,” Cambridge University Press, 1989.
- [28] M. Djordjevic, Phys. Rev. C **74**, 064907 (2006).
- [29] B. Blagojevic, M. Djordjevic and M. Djordjevic, Phys. Rev. C **99**, 024901 (2019).
- [30] M. Djordjevic, Phys. Rev. C **80**, 064909 (2009).
- [31] M. Djordjevic and U. W. Heinz, Phys. Rev. Lett. **101**, 022302 (2008).
- [32] M. Djordjevic and M. Djordjevic, Phys. Lett. B **734**, 286-289 (2014).
- [33] M. Djordjevic and M. Djordjevic, Phys. Lett. B **709**, 229-233 (2012).
- [34] S. Stojku, J. Auvinen, L. Zivkovic, P. Huovinen and M. Djordjevic, Phys. Lett. B **835**, 137501 (2022).
- [35] S. Stojku, B. Ilic, I. Salom and M. Djordjevic, Phys. Rev. C **108**, 044905 (2023).
- [36] Z. B. Kang, I. Vitev and H. Xing, Phys. Lett. B **718**, 482-487 (2012).
- [37] R. Sharma, I. Vitev and B. W. Zhang, Phys. Rev. C **80**, 054902 (2009).
- [38] M. Cacciari, S. Frixione, N. Houdeau, M. L. Mangano, P. Nason and G. Ridolfi, JHEP **10**, 137 (2012).
- [39] M. Djordjevic and M. Gyulassy, Phys. Rev. C **68**, 034914 (2003).
- [40] A. Peshier, [arXiv:hep-ph/0601119 [hep-ph]].
- [41] S. Borsányi, Z. Fodor, S. D. Katz, A. Pásztor, K. K. Szabó and C. Török, JHEP **04**, 138 (2015).
- [42] H. Niemi, G. S. Denicol, H. Holopainen and P. Huovinen, Phys. Rev. C **87**, 054901 (2013).
- [43] A. M. Sirunyan *et al.* [CMS], Phys. Lett. B **776**, 195-216 (2018).
- [44] V. Khachatryan *et al.* [CMS], JHEP **04**, 039 (2017).
- [45] S. Acharya *et al.* [ALICE], JHEP **11**, 013 (2018).
- [46] S. Acharya *et al.* [ALICE], JHEP **07**, 103 (2018).
- [47] M. Aaboud *et al.* [ATLAS], Eur. Phys. J. C **78**, 997 (2018).
- [48] [ATLAS], ATLAS-CONF-2017-012.
- [49] D. Zigic, J. Auvinen, I. Salom, M. Djordjevic and P. Huovinen, Phys. Rev. C **106**, 044909 (2022).
- [50] Code available at [21]
- [51] Because of the large error bars and low statistics we do not pay attention to the v_3 data above $p_{\perp} \approx 10$ GeV.
- [52] We remind the reader that in [14], we studied the early expansion using both free streaming and

fluid dynamics, and the results were the same: Early transverse expansion strongly reduces high- p_{\perp} v_2 irrespectively whether the expansion is fluid dynamical or not.